Immunity, Vol. 8, 319–329, March, 1998, Copyright ©1998 by Cell Press

Crystal Structures of Two I-A^d–Peptide Complexes Reveal That High Affinity Can Be Achieved without Large Anchor Residues

C. A. Scott,* P. A. Peterson,§ L. Teyton,† and I. A. Wilson*‡‖
*Department of Molecular Biology
†Department of Immunology
‡The Skaggs Institute of Chemical Biology
The Scripps Research Institute
10550 North Torrey Pines Road
La Jolla, California 92037
§R. W. Johnson Pharmaceutical Research Institute
3535 General Atomic Court
San Diego, California 92121

Summary

We have determined the structures of I-A^d covalently linked to an ovalbumin peptide (OVA$_{323–339}$) and to an influenza virus hemagglutinin peptide (HA$_{126–138}$). The floor of the peptide-binding groove contains an unusual β bulge, not seen in I-E and DR structures, that affects numerous interactions between the α and β chains and bound peptide. Unlike other MHC–peptide complexes, the peptides do not insert any large anchor residues into the binding pockets of the shallow I-A^d binding groove. The previously identified six-residue "core" binding motif of I-A^d occupies only the P4 to P9 pockets, implying that specificity of T cell receptor recognition of I-A^d–peptide complexes can be accomplished by peptides that only partially fill the MHC groove.

Introduction

Class II major histocompatibility complex (MHC) molecules are type I membrane glycoproteins that bind peptide fragments derived from exogenous protein sources, including viral and bacterial pathogens, and transport them to the cell surface for recognition by helper T cells (reviewed by Cresswell, 1994). Unlike class I MHC molecules, class II MHC molecules are found only on a limited number of cell types. These specialized antigen-presenting cells express three genetically distinct isotypes of class II MHC molecules in humans (HLA-DR, HLA-DQ, and HLA-DP), and two in mice (I-E and I-A). At present, structural information on class II MHC molecules is restricted to the HLA-DR isotype (Brown et al., 1993; Stern et al., 1994; Ghosh et al., 1995; Jardetzky et al., 1996; Dessen et al., 1997; Murthy and Stern, 1997) and its murine homologue, I-E (Fremont et al., 1996). Based on protein sequence comparisons, HLA-DQ and its murine homologue I-A are anticipated to have overall structures similar to I-E and DR molecules, but to differ in a number of important structural details (Brown et al., 1988; Brown et al., 1993; Paliaksis et al., 1996). Since strong genetic associations with autoimmunity have been established between certain alleles of HLA-DQ and I-A molecules (Campbell and Milner, 1993; Tisch and McDevitt, 1996), it is of great interest to determine whether any specific structural features of this important family can be correlated with autoimmune disease.

For most class I and class II MHC molecules, specific positions (anchor residues) in the bound peptide are conserved but differ from one MHC molecule to the next (reviewed by Rammensee et al., 1995). These peptide positions usually interact with specific pockets in the peptide-binding groove of the MHC molecule that accommodate peptide side chains of only a certain size and charge (Saper et al., 1991; Matsumura et al., 1992). In general, the anchor residues in peptides bound by class II MHC molecules, as for those bound by class I, are located within a nine-residue "core" motif (Rammensee et al., 1995). DR3, for example, has a hydrophobic residue (leucine, isoleucine, phenylalanine, methionine, or valine) at the first position of the nine-residue motif, aspartic acid at the fourth position, and tyrosine, phenylalanine, or leucine in the ninth position. Surprisingly, peptides that bind to certain alleles of I-A, such as I-A^d and I-A^b, do not appear to have as clearly identifiable nine-residue sequence binding motifs (Rammensee et al., 1995), implying that the requirement for their MHC class II pocket interactions may not be as stringent as for other class II MHC molecules.

OVA$_{323–339}$ is responsible for 25%–35% of the T cell response in BALB/c mice immunized with whole ovalbumin (Shimonkevitz et al., 1984) and has been extensively used to study the nature of class II MHC–peptide binding and T cell activation (Sette et al., 1987). HA$_{126–138}$ is an immunodominant peptide of influenza virus hemagglutinin that binds to I-A^d (Gerhard et al., 1991), and the I-A^d–HA complex is recognized by the T2.5-5 T cell receptor (TCR) transgenic mouse (Scott et al., 1994). The OVA and HA peptides form stable complexes with I-A^d. Dissociation of I-A^d–OVA complexes is nearly monophasic at 37°C, with a half-life of 33 hr (Witt and McConnell, 1994). HA has similar affinity for I-A^d (Sette et al., 1989b).

We have expressed soluble I-A^d in a recombinant form (Scott et al., 1996) and extended this work to produce I-A^d with either the OVA$_{323–339}$ (ISQAVHAAHAEINEAGR) or the HA$_{126–138}$ (HNTNGVTAASSHE) peptide attached by a six-residue linker (GSGSGS) to the first residue of the I-A^d β chain (Scott et al., 1998), as first described for I-E^k and I-A^d by Kappler and coworkers (Kozono et al., 1994; reviewed by Wilson, 1994). In this report, we describe the crystal structures of I-A^d–OVA and I-A^d–HA that have been determined at 2.6 and 2.4 Å resolution, respectively.

Results

Summary of Distinctive Structural Features of I-A^d

As seen in previously studied MHC molecules, the I-A^d peptide-binding site is formed by two long antiparallel α-helical segments that sit on top of and traverse an eight-stranded antiparallel β sheet. The most unusual

‖To whom correspondence should be addressed (e-mail: wilson@scripps.edu).

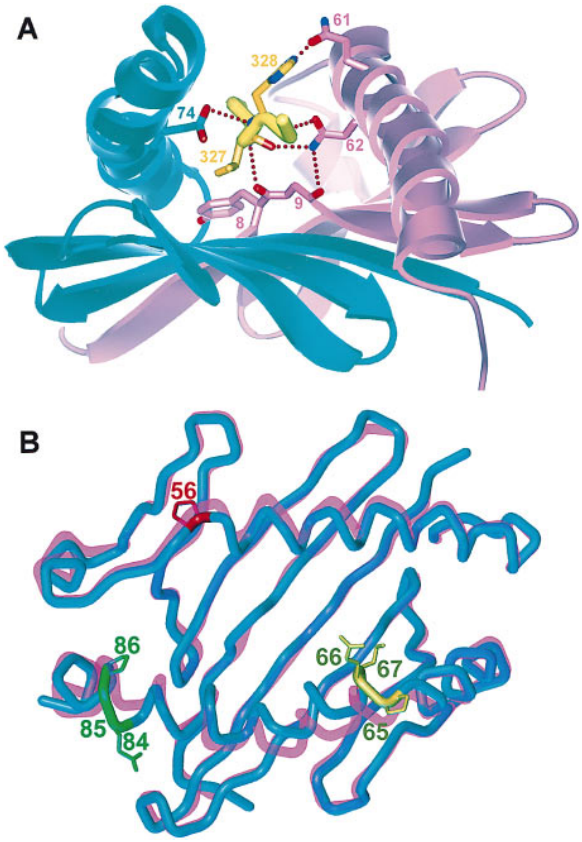

Figure 1. Unusual Features of the I-A^d Peptide-Binding Groove

(A) A view is shown along the I-A^d peptide-binding groove (from C to N of the peptide) to highlight the interaction of the β bulge, located in the β-sheet floor of the peptide-binding groove, with the central portion of the peptide (yellow). The α subunit is represented in magenta and the β subunit in cyan. Surprisingly, despite the bulge, the peptide is pulled deeper into the groove via H bonds with the main-chain atoms of the β-bulge residues, unimpeded in its downward movement because a glycine residue is used at the center of the bulge. The OVA-specific H bond between residue α61Gln and the P5 histidine residue of the peptide is also shown.

(B) Tertiary structure differences between I-A^d (cyan) and HLA-DR1 (magenta). The structure is viewed into the peptide-binding groove to show the inward movement of the I-A^d α helices compared to DR1. Proline α56 (red) may contribute to the helix movement in the α chain of I-A^d. The location of the polymorphic β65–β67 region (Pro65–Glu66–Ile67) is shown in yellow, close to another inward movement of the β_2 H2a helix. The π-helix segment (green) allows the insertion of β84Glu into the β_1 H2b helix.

feature of the I-A^d structure is a bulge in the floor of the peptide-binding groove, due to the insertion of an I-A/DQ–specific glycine in the first strand of the α chain. The β bulge makes a number of interactions that draw the central portion of both peptides deeper into the peptide-binding groove compared to DR– and I-E–peptide structures. The presence of I-A–specific polymorphism in the two α-helical walls of the peptide-binding groove appears to narrow the groove. Residues shown to be involved in I-A^d mismatched chain pairing are located primarily at the interface of the α and β subunits on the floor of the peptide-binding groove in the vicinity of the distinctive β bulge.

Two striking features relate to the alignment of the peptides in the MHC groove. First, neither peptide uses large side-chain residues to anchor the peptide into the peptide-binding groove. In both complexes, the key interaction appears to be insertion of a valine side chain into the central P4 pocket of the MHC molecule, a finding in full agreement with peptide-binding studies. Second, with one exception, all hydrogen bonds (H bonds) between I-A^d and peptide are to the peptide backbone, revealing an essentially sequence-independent H bond network.

Overall Structure of the Complexes

The α and β polypeptide main chains of I-A^d are similar in their overall fold to those previously reported for human and mouse class II MHC molecules. Thirteen residues of each covalently attached peptide had interpretable electron density. The amino-terminal domains of each chain, α_1 and β_1, form a characteristic peptide-binding groove that was initially described for human (Bjorkman et al., 1987) and mouse (Fremont et al., 1992) MHC class I molecules (Figure 1). The I-A^d β_2 domain is moderately rotated, compared to other class II structures, with a main-chain root-mean-square deviation (rmsd) as large as 4 Å. The putative CD4 binding site, residues β137–β143 (König et al., 1992), has a conformation that is similar to that of previous class II structures. The top surface of the α helices of the I-A^d peptide-binding groove, which would be accessible for interaction with the TCR, appears electrostatically neutral, similar to the DR1 helices and in contrast to the electronegative properties of the I-E^k helices.

The OVA and HA peptides are bound to I-A^d in an extended type II polyproline conformation (Figure 2), as previously observed in other class II structures (reviewed by Wilson, 1996), with an rmsd of 0.75 Å for all corresponding peptide main-chain atoms. Two additional residues (Arg-Gly) from the signal sequence remain connected to the amino terminus of each peptide. The covalent linker attaching the peptide to the β chain is disordered in both complexes. The OVA peptide sequence extends to the P−1 position, with additional density for a glycine from the signal sequence at the P−2 position and main-chain density for an arginine at the P−3 position (which was modeled as an alanine residue). The HA peptide sequence extends to the P−2 position with density for the signal sequence glycine visible at the P−3 position. The first two residues of the HA peptide are raised as a result of being a crystal contact for a symmetry-related I-A^d–HA molecule. At the other end, electron density is visible for residues up to the P11 position and accounts for all of the $HA_{126–138}$ residues but only 12 ($OVA_{323–334}$) of the 17 $OVA_{323–339}$ residues. Approximately 66% of the HA peptide surface area is buried by I-A^d (744 Å^2 of 1118 Å^2; probe radius 1.7 Å), and 70% of the OVA peptide (800 Å^2 of 1152 Å^2), comparable with other class II MHC–peptide complexes, which range from 62% (I-E^k-Hsp) to 70% (DR3-CLIP; Ghosh et al., 1995).

The I-A^d Peptide-Binding Groove

The most distinctive feature of the I-A^d structure, compared to the other class II HLA-DR and I-E molecules,

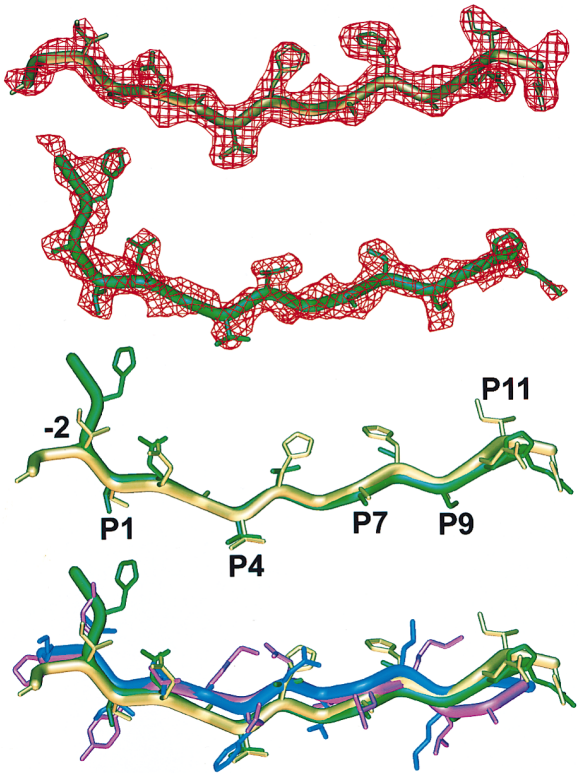

Figure 2. OVA and HA Peptide Electron Density and Conformation

(Top) The $F_o - F_c$ shake-omit density maps are contoured at a 3 σ level for the OVA (gold) and HA (green) peptides, with the final refined peptides coordinates superimposed. (Bottom) A comparison of the HA and OVA peptides bound to I-A^d, with peptides bound to other class II MHC–peptide structures: the HA peptide (magenta) from the DR1–HA complex (Stern et al., 1994), and the Hb peptide (blue) from the I-E^k–Hb complex (Fremont et al., 1996). The I-A^d–bound peptides lie deeper in the groove than other class II bound peptides and have smaller downward-pointing side chains that anchor these peptides to the MHC molecule.

is the presence of a β bulge on the β-sheet floor of the peptide-binding domain (Figure 1A). The β bulge is located in the first strand of the β sheet of α_1, at the base of the P4 pocket. The β bulge is formed by two residues that protrude above the β sheet: α8Tyr replaces a highly conserved α9Gln seen in the DR and I-E family of MHC structures, and α9Gly is an inserted residue not seen in previous class II structures. An H bond is formed between the main-chain carbonyl oxygen (O) of α8Tyr and the main-chain nitrogen (N) of the peptide P4 residue (Val327 in Figure 1A) and replaces two H bonds made to the P4 residue of the peptide by the α9Gln seen in the DR1 and I-E^k structures. The outcome is a network of H bonds that pulls the central (P2–P8) region of the I-A^d peptides deeper into the peptide-binding groove. Sequence comparisons suggest that the β bulge will be a conserved feature of I-A and HLA-DQ molecules.

The two long helical segments of I-A^d, which form the walls of the binding groove, are closer together and present a narrower groove than is seen in other class II structures (Figure 1B). The inward movement of both helices appears to be due to the acquisition of particular proline residues and other side chains in the α-helical segments, which are not present in DR and I-E molecules. The I-A^d α_1 helical axis (α56–α77) is translated inward, toward the center of the binding site, by as much as 1.2 Å relative to the DR1–HA complex. This movement appears to be at least partially attributable to the constrained geometry of a proline at residue α56, unique to I-A and DQ molecules, which is used as an α-helix initiation site. The inward movement of the α helix is stabilized by an I-A–specific H bond between the carbonyl O of the β-bulge α9Gly and the NHδ2 of α62Asn in the α_1 helix (Figure 1A). Mutation of α56Pro of I-A^k to alanine results in a loss of peptide-binding ability (Nelson et al., 1996). Other MHC-like structures, such as the neonatal Fc receptor (Burmeister et al., 1994) and CD1 (Zeng et al., 1997), have proposed proline-related movement of α-helical segments that are amino-terminal to the proline.

A number of distinctive features in the segmented β_1 helices of I-A^d also contribute to alteration of the peptide-binding groove. Relative to DR1, the orientation of the I-A^d H2a segment (β65–β77) is translated inward by as much as 2.6 Å in the vicinity of another proline at position β65. Residues β67Ile and β71Thr, which form one side of the P7 pocket, have smaller side chains compared to I-E^k residues, β67Phe and β71Lys, and allow unimpeded inward movement of the I-A^d β_1 H2a α helix. Since DQ molecules lack β65Pro, it is anticipated that they will have an H2a helix position more similar to that seen in the DR structures, which also lack a proline at β65.

Residue β65Pro is also the first residue in a serologically immunodominant three-residue segment that is polymorphic among I-A alleles (Buerstedde et al., 1989). In I-A^d, and other alleles such as I-A^b, this segment is Pro65–Glu66–Ile67. The most common polymorphism has deletions at both β65 and β67, and a Tyr at β66, as seen in I-A^k and I-A^{g7}. In I-A^d, residues β65Pro and β66Glu project upward from the α helix and are likely sites for TCR interaction, consistent with a report that residues β65-β67 are necessary for recognition of I-A^d–OVA by the T cell hybridoma DO-11.10 but do not control specificity of peptide binding to I-A^d (Lee et al., 1991). Residue β67Ile projects sideways into the groove and forms the boundary of the shallow P7 pocket.

The most dramatic change in the β_1 helix occurs at the end of the H2b segment, β79–β84. The presence of a proline at position β86 prevents a standard 3.6_{13} α-helical H bond to position β82, as seen in other class II structures. Instead, the carbonyl O at position β82 now accepts an H bond from the backbone N at position β87, and similarly β83 H bonds to β88, thus forming a short 4.4_{16}, or π helix, that creates a kink between residues β82 and β88. Within this π helix, a conformationally flexible glycine at β85 allows for insertion of a Glu at residue β84, compared to DR and I-E structures. Alignment of class II β chain sequences predicted that this insertion would occur further along in the chain at the β strand connecting the β_1 and β_2 domains (Klein, 1986). However, the sequence register of the H3 helix can be changed such that the insert occurs much earlier, at residue 84. Residue β84Glu is located on the outer side of the H2b segment. The β85Gly–β86Pro sequence is found in a number of I-A alleles, including I-A^d and I-A^b, but not I-A^k.

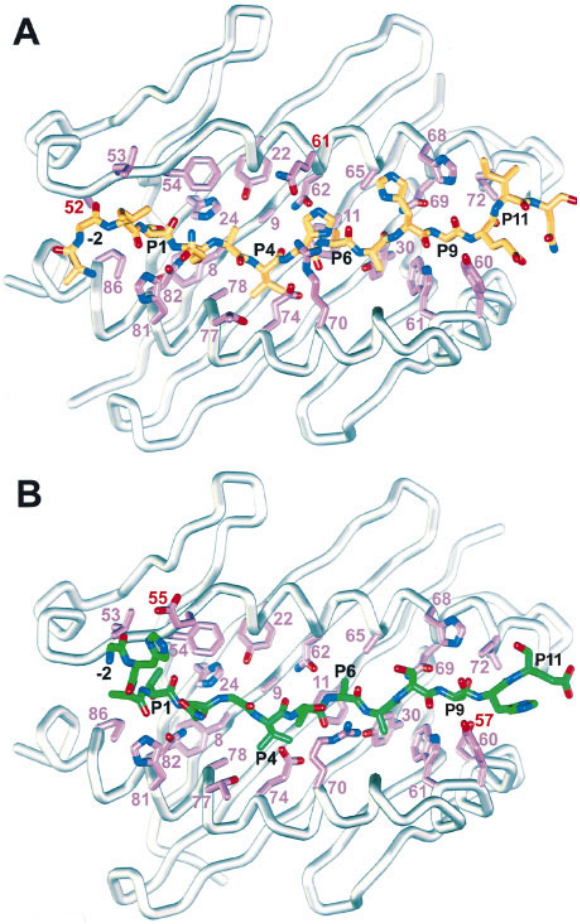

Figure 3. Interactions of the OVA and HA Peptides with I-A^d

All residues that are in van der Waals contact with both OVA (A) and HA (B) are numbered in pink. The Cα backbone of the I-A^d peptide-binding domain is represented by the gray tube. I-A^d side-chain interactions that are specific to each peptide are labeled in red.

Fewer Interactions between I-A^d and Peptide

With few exceptions, I-A^d uses the same residues to interact with each peptide (Figure 3 and Table 1). I-A^d forms fewer backbone H bonds to the bound peptide compared to DR1 (Stern et al., 1994), DR3 (Ghosh et al., 1995), and I-E^k (Fremont et al., 1996) class II–peptide complexes, and is comparable to the recent structure of a DR4-CII complex (Dessen et al., 1997). With one exception, all H bonds between I-A^d and peptide are to the peptide backbone. Fifteen H bonds are made between I-A^d and OVA and 14 H bonds between I-A^d and HA. Fourteen H bonds involve MHC residues that are highly conserved in I-A sequences (Figure 4); 10 of these H bonds involve I-A^d residues that are conserved in most human and mouse class II proteins (Stern and Wiley, 1994). The other four H bonds—P4 N to the main-chain O of α8, P5 N to Oϵ β74Glu, P7 N to OHη of β30Tyr, and P9 O to Nϵ2 of α68His—involve residues that are conserved in all I-A and most DQ molecules.

In both I-A^d–peptide structures, β57Asp forms an interchain salt bridge to α76Arg, which is essential for proper peptide binding and efficient surface expression (Nalefski et al., 1995). Surprisingly, β57Asp of I-A^d does not form any H bonds, either directly or through water molecules, to the backbone of the HA and OVA peptides. In contrast, a direct H bond between β57Asp and peptide is seen in the HLA-DR1 and DR3 peptide complexes (Stern et al., 1994; Ghosh et al., 1995; Murthy and Stern, 1997), while a water-mediated H bond between β57Asp and peptide is seen in the I-E^k–Hb complex (Fremont et al., 1996). In the I-A^d–HA complex, a water-mediated H bond is seen between α76Arg and peptide, instead of a direct α76Arg-to-peptide H bond seen in other HLA-DR1, DR3, and I-E^k class II MHC–peptide complexes. The altered H bond pattern between I-A^d and the carboxy-terminal region of the peptide appears to be caused by a shallow P9 pocket and a new H bond between α68His and the P9 O of the peptide, which together force the peptide main chain to sit higher in the peptide-binding groove. We cannot, however, exclude the possibility that the lack of H bonds is affected by tethering of the peptide by a covalent linker. Collectively, these observations indicate that the primary role of β57Asp is to stabilize the I-A^d $\alpha\beta$ heterodimer while not making any direct contribution to stabilization of the bound peptide.

The nature of the sequestered environment in and around the P4 pocket is completely changed by the presence of the β bulge; no water molecules are buried in the I-A^d–HA complex that could establish the pH-dependent H bond network seen in the I-E^k complexes (Fremont et al., 1996). The I-A^d–OVA complex was crystallized at pH 5.5 and the I-A^d–HA complex at pH 7.4. The structure of the P4 pocket is essentially the same for both complexes. Thus, we are led to the conclusion that the modulation of I-A^d peptide binding cannot be rationalized by the formation of pH-dependent H bond networks within the P4 pocket. This observation may be relevant to previous results that showed that optimal peptide binding by I-A^d occurs at a higher pH than for I-E^d, I-E^k, and I-A^k (Runnels et al., 1996).

Peptide-Binding Motif of I-A^d

The I-A^d peptide-binding groove has only one moderately large pocket, P1, between the main-chain atoms of the peptide and the peptide-binding groove surface (Figure 5). Three smaller cavities, corresponding to the P4, P6, and P9 pockets, can also be identified. The pocket structure of the I-A^d peptide-binding groove differs markedly from that of the I-E^k binding groove, where the P4 and P9 pockets are the predominant sites occupied by large peptide side-chain anchors (Figure 6). Unlike the DR1–HA structure, the largest pocket of I-A^d accommodates peptide residues that only partially fill the P1 pocket.

Grey and coworkers have carried out extensive studies to identify the binding motif of I-A^d (Sette et al., 1987, 1988, 1989a, 1989b, 1989c, 1990; Hunt et al., 1992). The core motif was proposed to be only six residues in length, with the first, third, and fourth residues being hydrophobic and the sixth residue generally being an alanine or serine. In the I-A^d crystal structure, the six-residue core motif is positioned such that it extends from the P4 pocket to the P9 pocket (Figure 5 and Table 2). In the I-A^d–OVA complex, the large P1 pocket is occupied only partially by Ser324, and the third-largest

Table 1. H Bonds and van der Waals Interactions between I-A^d and the HA and OVA Peptides

	Hydrogen Bonds		van der Waals				
P−2	HA (His)	α**55Glu** (Oε2←NHδ1[a])		α53Leu	α**55Glu**		
	OVA (Gly[b])	α53Leu (NH→O)	α52Ala	α53Leu			
P−1	HA (Asn[c])	β81His (NHε2→O)	α53Leu	β81His			
	OVA (Ile)	β81His (NHε2→O)	α53Leu	β81His			
P1	HA (Thr)	α53Leu (O←NH)	α54Phe	β82Asn	β86Pro		
	OVA (Ser)	α53Leu (O←NH)	α54Phe	β82Asn	β86Pro		
P2	HA (Asn)	β82Asn (Oδ1→NH), (NHδ2→O)		β77Thr		β81His	β82Asn
	OVA (Gln)	β82Asn (Oδ1←NH), (NHδ2→O)	α24His	β77Thr	β78Ala	β81His	β82Asn
P3	HA (Gly)		α**8Tyr**	α22Tyr	α**24His**	α54Phe	
	OVA (Ala)		α**8Tyr**	α22Tyr	α**24His**	α54Phe	β78Ala
P4	HA (Val)	α**8Tyr(OHη←NH)**, α62Asn(NHδ2→O)	α**8Tyr**	α9Gly	β**11Phe**	β74Glu	β78Ala
	OVA (Val)	α**8Tyr(OHη←NH)**, α62Asn(NHδ2→O)	α**8Tyr**	α9Gly	β**11Phe**	β**28Thr**	β74Glu
P5	HA (Thr)	β**74Glu(Oε←NH)**		α62Asn	β**11Phe**	β**70Arg**	β**74Glu**
	OVA (His)	β**74Glu(Oε←NH)**, α**61Gln (Oε1←NHε2)**	α**61Gln**	α62Asn	β**11Phe**	β**70Arg**	β**74Glu**
P6	HA (Ala)	α62Asn(Oδ1←N)	α62Asn	α65Ala	β11Phe	β30Tyr	
	OVA (Ala)	α62Asn(Oδ1←N)	α62Asn	α65Ala	β11Phe		
P7	HA (Ala)	α69Asn (NHδ2→O), β**30Tyr (OHη←NH)**		β**30Tyr**	β61Trp		
	OVA (Ala)	α69Asn (NHδ2→O), β**30Tyr (OHη←NH)**	α69Asn	β**30Tyr**	β61Trp		
P8	HA (Ser)	β61Trp(NHε1→O)			α69Asn		β61Trp
	OVA (His)	β61Trp(NHε1→O)	α65Ala	α68His	α69Asn	β60Tyr	β61Trp
P9	HA (Ser)	α69Asn(Oδ1←NH), α**68His(NHε2→O)**	α**68His**	α69Asn	α72Ile	β57Asp	β61Trp
	OVA (Ala)	α69Asn(Oδ1←NH), α**68His(NHε2→O)**	α**68His**	α69Asn	α72Ile		β60Tyr
P10	HA (His)		α72Ile	β60Tyr			
	OVA (Glu)		α72Ile	β60Tyr			
P11	HA (Glu)						
	OVA (Ile)		α68His	α72Ile			

Residues in bold indicate interactions seen in I-A^d that are not present in previous class II–peptide structures. Underlined residues indicate that other MHC class II molecules use this residue position but with a different side chain making contact with peptide.
[a] Hydrogen bonds are indicated from I-A^d atom to peptide atom. The direction of the arrow indicates donor→acceptor.
[b] Residue is from signal peptide sequence.
[c] Built as an alanine because no side-chain density is visible.

pocket, the P9 pocket, is filled only partially by Ala332. Val327 sits firmly in the P4 pocket anchoring the peptide register (Figure 6). The last four residues of the 17-mer OVA peptide, OVA$_{336–339}$, are not visible in the electron density map and presumably do not make any well-defined contacts with I-A^d, consistent with a report that OVA$_{323–335}$ binds to I-A^d with an affinity equal to that of OVA$_{323–339}$ (Sette et al., 1987). The I-A^d–HA complex exhibits a similar pattern of binding, with its core motif also

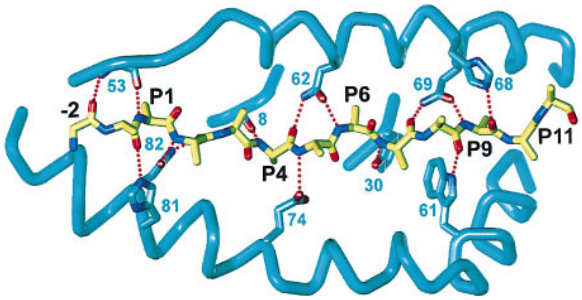

Figure 4. The Conserved H Bonds between I-A^d and the Peptide Backbone

The H bonds occurring between the main-chain O of the β bulge and the P4 N of the peptide are partially obscured by peptide. For clarity, only the α helices and fragments of the β structure are shown.

sitting between the P4 and P9 pockets. The HA peptide partially fills the P1 (Thr128) and P9 (Ser135) pockets, with Val131 providing the only obvious side chain anchor into the P4 pocket (Figure 5). Ser135 appears to compensate for not filling the P9 pocket by forming a long H bond (3.5 Å) between its OHγ and Oδ1 of αAsn69. αAsn69 is a key residue that interacts with the peptide backbone at P7 and P9 (Figure 4). Small P9 residues have been observed in the DR4-CII complex (glycine; Dessen et al., 1997) and I-A^k–HEL (serine; Fremont et al., 1998 [this issue of *Immunity*]). The six-residue covalent linker is long enough to allow the 13-mer HA peptide to occupy the entire MHC peptide-binding groove. The OVA peptide has four additional residues compared to the HA peptide and therefore should be able to interact in all possible registers with the I-A^d groove. Consequently, the register that we observe in the I-A^d–OVA complex should represent the most energetically favored register adopted by the OVA$_{323–339}$ peptide.

Residue Differences That Affect Mismatched Allele Dimerization

The I-A^d β chain is particularly promiscuous in its ability to dimerize with α chains and has been shown to form mixed dimers with I-A^b, I-A^k, I-E, DR, DQ, and DP α chains, whereas I-A^b and I-A^k β chains will form mixed dimers only with other I-A α chains (Lechler et al., 1990).

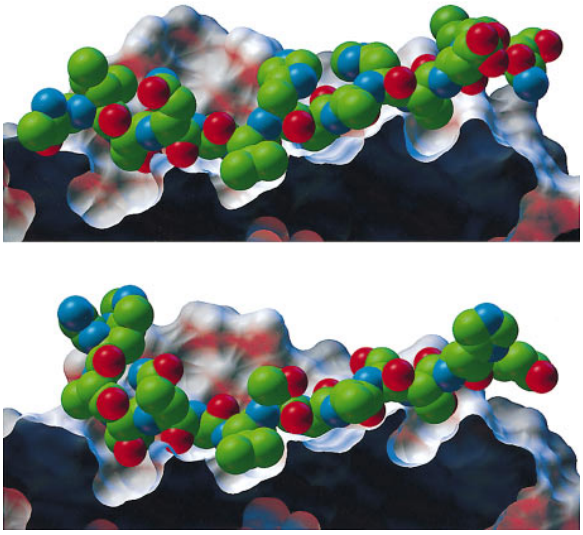

Figure 5. The Peptide-Binding Pockets of I-A^d

A side view and a cross-section of the I-A^d–OVA (top) and I-A^d–HA (bottom) complexes, showing the location of partially filled MHC pockets. The peptide amino terminus is at the left. The central valine at the P4 pocket in both complexes appears to fix the register for the peptide. The P1 and P9 pockets are not filled by the OVA and HA sequences.

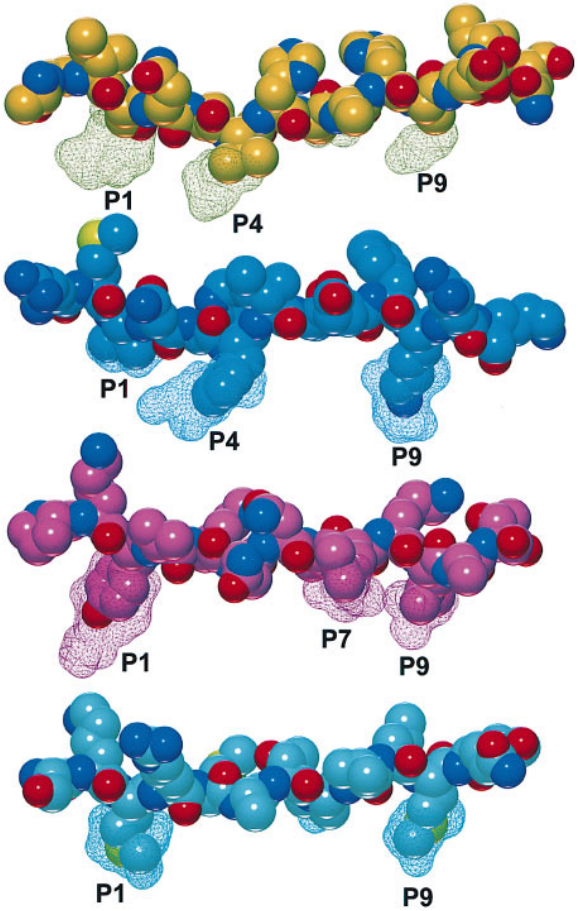

Figure 6. Comparison of Class II MHC Molecule Binding Pocket Structure

The location, size, and occupancy of the pockets in the peptide-binding groove of I-A^d in comparison with other class II MHC–peptide structures: I-A^d–OVA complex (gold), I-E^k–Hsp complex (blue), DR1–HA complex (magenta), and DR3-CLIP (cyan). Both I-E and I-A molecules use a prominent P4 pocket, in contrast to the DR molecules. In contrast to the other MHC molecules, I-A^d does not use its largest pocket, located at P1, to anchor the OVA peptide into the peptide-binding groove. The coordinates used were I-E^k–Hsp (Fremont et al., 1996; PDB accession code 1IEB), DR1–HA (Stern et al., 1994; PDB accession code 1DLH), and DR3-CLIP (Ghosh et al., 1995; provided by Partho Ghosh and Don Wiley).

As previously suggested (Lechler et al, 1990; Sant et al., 1991 and references therein), the I-A^d structure reveals that certain residues present in the first strand of the β_1 domain play a direct role in dimerization (Figure 7). First, β12Lys projects down from the β sheet and makes an interchain H bond with the main-chain carbonyl O of α140 in the α_2 domain. I-A^k and I-A^b have glutamine and methionine at β12, respectively, and are predicted not to make this H bond. Second, residue I-A^d β9Val interacts with the α_1 helix at polymorphic residue α66Glu. In I-A^b and I-A^k β9 is a tyrosine and histidine, respectively. Consequently, the β chains of I-A^b and I-A^k will pack correctly only with α chains having a small side chain (valine or glycine) at residue α66, whereas the I-A^d β chain is able to interact with all α chains without a steric clash with residue α66. Third, the conformationally flexible β13Gly sits adjacent to the β bulge in the first strand of α_1 at the base of the P4 pocket. Residue β13 is an inflexible proline in I-A^k that most likely alters the β-sheet structure in and around the β bulge. Fourth, β14Glu forms two H bonds with β16Tyr and β29Arg that appear to stabilize the β-sheet structure of the β_1 domain.

Discussion

The peptide interactions in the I-A^d–OVA structure are in full agreement with the experimentally derived binding data of Grey and coworkers (Sette et al., 1987). The two residues that were shown by mutagenesis to be most important for I-A^d binding, Val327 and Ala332, are oriented downward into the P4 and P9 pockets. These pockets can accommodate small, uncharged peptide side chains, and mutation of these residues to larger or charged groups greatly reduces peptide binding (Sette et al., 1987). Val327 of the I-A^d–OVA complex is almost fully buried in the P4 pocket and is making the key hydrophobic interaction that sets the register of the peptide within the groove. No clear residue motif has been determined for the P1 residue of I-A^d, implying that occupancy of this pocket by residues of specific size and charge is not necessary for high-affinity peptide binding. This agrees with our observations that neither the OVA (Ser324) nor the HA (Thr128) peptide side chain fills the P1 pocket. Ala326 (P3), Ala329 (P6), and Ala330 (P7) are oriented sideways or slightly upward and establish a hydrophobic surface in the center of the peptide-binding groove. Replacement of these residues with larger side chains does not affect peptide binding to I-A^d but does hinder T cell recognition, consistent with the fact that any further extension at the β carbon would have to project upward from the peptide-binding groove. The

Table 2. Register of Full-Length and Truncated OVA and HA Peptides within the Pocket Structure of the I-A^d Peptide-Binding Groove

				Peptide Register																			
				P −3	P −2	P −1	P 1	P 2	P 3	P 4	P 5	P 6	P 7	P 8	P 9	P 10	P 11						
Core motif[a]										h		h	h		*								
HA$_{126–138}$[b]				**G**	**H**	**N**	**T**	**N**	**G**	**V**	**T**	**A**	**A**	**S**	**S**	**H**	**E**						
HA$_{128–138}$ (2.0)[c]							T	N	G	V	T	A	A	S	S	H	E						
HA$_{126–136}$ (0.5)[c]					H	N	T	N	G	V	T	A	A	S	S								
OVA$_{323–339}$[b]				**R**	**G**	**I**	**S**	**Q**	**A**	**V**	**H**	**A**	**A**	**H**	**A**	**E**	**I**	**N**	**E**	**A**	**G**	**R**	
OVA$_{327–339}$ (0.3)[d]										V	H	A	A	H	A	E	I	N	E	A	G	R	
OVA$_{323–332}$ (0.2)[d]						I	S	Q	A	V	H	A	A	H	A								
Myo$_{108–118}$ (8.0)[e]						S	E	A	I	I	H	V	L	H	S	R							
Nase$_{101–114}$[f]							E	A	L	V	R	Q	G	L	A	K	V	A	Y				
λ rcpt$_{12–26}$ (1.0)[g]							L	E	D	A	R	R	L	K	A	I	Y	E	K	K	K		
Apo-E$_{270–283}$ (0.4)[h]			W	A	N	L	M	E	K	I	Q	A	S	V	A	T	N	P	I				
YT core (10.0)[i]						Y	T	Y	T	V	H	A	A	H	A	Y	T	Y	T				
YTA core (7.1)[i]							Y	T	A	V	H	A	A	H	A	A	Y	T					
AM core (6.3)[i]						A	M	A	M	V	H	A	A	H	A	A	M	A	M				
AK core (4.6)[i]						A	K	A	K	V	H	A	A	H	A	A	K	A	K				
ROI (27.7)[j]				V	H	A	A	H	A	V	H	A	A	H	A	V	H	A					
ROIV (34.0)[j]				A	H	A	A	H	A	A	H	A	A	H	A	A	H	A	A				
OVA alt 1	I	S	Q	A	V	H	A	A	H	A	E	I	N	E	A	G	R						
OVA alt 2				I	S	Q	A	V	H	A	A	H	A	E	I	N	E	A	G	R			

The register of HA$_{126–138}$ and OVA$_{323–339}$ (bold) was used to align other high-affinity peptides in the I-A^d peptide-binding groove. Immediately below the HA and OVA peptides are the proposed alignment of truncated HA and OVA peptides. The last two lines show two alternative (alt) alignments of OVA$_{323–339}$. The remaining lines show the possible alignment of other high-affinity peptides. Where known, the relative binding capacity of each peptide, compared to OVA$_{323–339}$ binding, is given in parentheses.

[a] h, hydrophobic; asterisk, A/S.
[b] Underlined residues are from signal sequence.
[c] Sette et al., 1988, 1989b.
[d] Sette et al., 1987.
[e] Sperm whale myoglobin (Sette et al., 1988; England et al., 1995).
[f] Staphylococcal nuclease (Sette et al., 1987, 1989a).
[g] λ phage receptor (Sette et al., 1989b).
[h] Mouse apolipoprotein (Hunt et al., 1992).
[i] Core extended-peptides (Sette et al., 1989c).
[j] High-affinity peptides (Sette et al., 1990).

two histidine residues, His328 (P5) and His331 (P8), along with the P−1 residue, project out from the MHC–peptide surface and are in excellent position to be T cell epitopes. Mutagenesis studies identified the His residues as critical for recognition by the T cell hybridomas 3DO-54.8 and 8DO-51.15 (Sette et al., 1987). The I-A^d–HA complex provides further independent verification that the register of the OVA peptide can be adopted by other peptides and is most likely a general feature of peptide binding by I-A^d.

The I-A^d–peptide structures can be used to predict the alignment of peptides known to bind I-A^d with high affinity (Sette et al., 1988, 1989a; Hunt et al., 1992). A sperm whale myoglobin peptide (MYO$_{102–118}$), for example, would be predicted to place Ser117 in the medium-sized P9 pocket, allowing the hydrophobic residue Ile112 to sit in the P4 pocket (Table 2). The predicted agretopes and epitopes of the MYO peptide agree with the conclusions derived from a mutational study of this complex and a structure-based alignment (England et al., 1995). As a second example, alignment of apolipoprotein-E$_{268–283}$ peptide (Hunt et al., 1992) and a high-affinity peptide that has an Ala–Met sequence repeated on each side of the core OVA motif (AM core) places a methionine in the P1 pocket (Table 2). The P1 pocket of I-A^d is large enough to accommodate the flexible methionine side chain. Mouse CLIP$_{85–101}$ has been extracted from purified I-A^d molecules (Hunt et al., 1992) and requires its methionine residues to bind I-A^d (Sette et al., 1995). In the DR3-CLIP x-ray structure (Ghosh et al., 1995), methionines occupy the P1 and P9 pockets. Although the P1 pocket of I-A^d appears to be large enough to accommodate a methionine, the P9 pocket of I-A^d is smaller than in DR3 (Figure 6), forcing Met98 of mouse CLIP to sit suboptimally in the P9 pocket. In agreement with this proposition, mutation of Met99 to alanine enhances the affinity of CLIP for I-A^d (Gautam et al., 1995).

For DR molecules, most of the peptide-binding energy is due to H bonds to the peptide backbone and the interaction of at least one large hydrophobic side chain anchor residue with an MHC pocket (Jardetzky et al., 1990; Hill et al., 1994). I-A^d also binds peptides using a number of H bonds to the peptide backbone, but unlike other class II MHC–peptide structures, OVA and HA bind I-A^d without the use of large side-chain anchor residues, reducing the amount of buried peptide surface area. Paradoxically, full occupancy of the P4 pocket appears

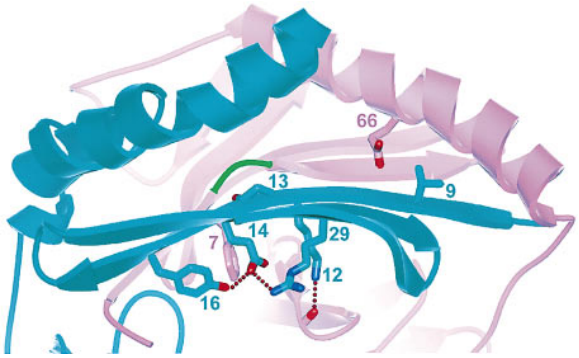

Figure 7. Structurally Important Residues in I-A^d $\alpha\beta$ Chain Dimerization

A side view of I-A^d, showing some of the principal residues that play a role in determining the degree of mixed $\alpha\beta$ chain pairing. Most of the residues identified are polymorphic within the I-A isotype. The α subunit is shown in magenta, and the β subunit is shown in blue. The β bulge is highlighted in green. The H2a helix of the β subunit has been omitted to reveal the close association of α66Glu with β8Val.

not to be an absolute requirement for peptide binding, since mutation of the OVA residue Val327 to alanine does not significantly reduce binding affinity for I-A^d (Sette et al., 1989a). These observations contrast with data from studies of the DR1–HA complex, in which mutation of the key anchor residue, Tyr308, to alanine severely reduced binding to DR1 (Jardetzky et al., 1990).

A number of natural (Hunt et al., 1992) and synthetic peptides (Sette et al., 1989c, 1990) have higher affinities for I-A^d than OVA$_{323–339}$. Alignment of most of these peptides sequences with the HA and OVA peptides indicates that increased binding occurs because the P1 pocket is now occupied by a larger peptide side chain (Table 2). However, certain synthetic peptides (ROI and ROIV) have a higher capacity to bind I-A^d than OVA$_{323–339}$. These peptides cannot fill the P1 pocket with a large side chain without the unfavorable introduction of a histidine residue into the P4 pocket (Table 2). Surprisingly, alternative alignments of these peptides will place alanines at the P1 and P9 pockets, filling the P4 pocket either with a valine or an alanine. It is possible, given the minimal side-chain requirements for peptide binding by I-A^d, that these alanine-rich synthetic peptides can be bound in a number of alternative registers, forming a mixed population of MHC–peptide complexes. Thus, while DR1 binds peptides that use a single large side-chain interaction to increase affinity, I-A^d selectively binds peptides with small, hydrophobic side chains that avoid steric clashes in the center of the binding groove.

Results from the I-A^d–peptide structures and a number of I-A^d–peptide-binding studies suggest that I-A^d readily binds peptides that only partially fill the peptide-binding groove. Alignment of the truncated peptide HA$_{128–138}$ with the six-residue I-A^d motif would place Thr128 in the P1 pocket, leaving empty the region of the peptide-binding groove that binds the P$-$1 and P$-$2 peptide residues (Table 2). Surprisingly, HA$_{128–138}$ binds to I-A^d with similar affinity as OVA$_{323–339}$ (Sette et al., 1988). Conversely, Ser136 of the 11-mer HA$_{126–136}$ would sit in the P9 pocket, leaving empty the P10 and P11 positions at the carboxy-terminal end of the binding groove (Table 2). HA$_{126–136}$ binds to I-A^d almost as well as OVA$_{323–339}$ (Sette et al., 1988). Similar logic can be applied to high-affinity, truncated sperm whale myoglobin peptides (Sette et al., 1988), high-affinity truncated λ phage repressor peptides (Sette et al., 1989b), and perhaps even the shorter OVA$_{324–334}$ peptide (Sette et al., 1989b). The implication is that I-A^d is able to bind peptides with high affinity without having the entire peptide-binding groove occupied. Truncation studies of the OVA$_{323–339}$ peptide reveal a further level of complexity. Truncated OVA$_{327–339}$ binds with approximately one third of the affinity of OVA$_{323–339}$. Consequently, either I-A^d binds the amino-terminal Val327 in the P4 pocket, leaving a large proportion of the binding groove empty, or OVA$_{327–339}$ binds I-A^d in alternative registers by placing suboptimal residues in the P4 and P9 pockets (Table 2).

A number of murine autoimmune diseases require expression of specific I-A alleles for disease onset. The best case is I-A^{g7}, associated with insulin-dependent diabetes mellitus (reviewed by Tisch and McDevitt, 1996) and more recently with murine rheumatoid arthritis (Kouskoff et al., 1996). Based on protein sequence comparison, I-A^{g7} should share strong structural similarity to I-A^d, since the α chain of I-A^d and I-A^{g7} are the same, and only 17 residues differ between the I-A^d and I-A^{g7} β chains, all located in the β_1 domain. The absence of a proline at β56 in I-A^{g7} would be predicted to destabilize the orientation of the H1 segment of the β_1 α helix. Replacement of the I-A^d β57Asp with the I-A^{g7} β57Ser would destroy the salt bridge between β57Asp and α76Arg and probably destabilize the $\alpha\beta$ dimer. Since these salt bridge residues also form direct or indirect H bonds to the peptide backbone, I-A^{g7} would be predicted to present peptides whose carboxy-terminal portion was loosely bound in the MHC groove. It is interesting that in HLA-DR4, an isotype specifically associated with rheumatoid arthritis, no backbone interactions are made with β57Asp or α76Arg (Dessen et al., 1997). The presence of a histidine at residue β9 in I-A^{g7}, instead of a valine in I-A^d, would require the β9 side chain to occupy the P4 pocket in order not to collide with α66Glu, a residue implicated in $\alpha\beta$ dimerization. Consequently, the P4 pocket used by I-A^d to align the HA and OVA peptides may be further reduced in size in I-A^{g7}, perhaps excluding its use as a site for anchoring peptide side chains. Finally, the replacement of the I-A^d tryptophan with the I-A^{g7} tyrosine at residue β61 will remove the ability to form an H bond to the peptide main chain O of the P8 residue that is important in class I and class II molecules (reviewed by Stern and Wiley, 1994). Thus, a number of residues that differ between I-A^d and I-A^{g7} are located at sites that are important for establishing proper $\alpha\beta$ chain dimerization and peptide binding in the I-A^d–peptide complexes.

Experimental Procedures

DNA Constructs, Protein Purification, and Crystallization

A leucine zipper–hexahistidine tail was added to the coding region for the extracellular domains of the I-A^d α and β chains as previously described (Scott et al., 1996). The I-A^d β chain DNA sequence was

Table 3. X-Ray Crystallographic Data and Statistics for the I-A^d–OVA and I-A^d–HA Structures

	I-A^d–OVA$_{323–339}$	I-A^d–HA$_{126–138}$
Crystallization conditions	32% PEG 600 0.1 M imidizole malate (pH 5.5)	19% PEG 8000 0.2 M Tris (pH 7.4)
Space group	$P4_12_12$	C2
Cell constants	a = b = 101.3 Å, c = 92.6 Å	a = 127.2 Å, b = 100.2 Å, c = 53.1 Å, β = 100.3°
R_{sym} (I)	5.7%	7.6%
Last shell	38.3% (2.7–2.6 Å)	25.9% (2.5–2.4 Å)
$F_o \geq 0\sigma$ no. (% completness)	14,777 (99%)	22,555 (89%)
Last shell	1,690 (91%)	2,820 (88%)
$F_o \geq 2\sigma$ no. (% completness)	14,001 (91%)	21,229 (83%)
Last shell	1,400 (75%)	2,390 (74%)
Protein + peptide atoms	α1–178, β6–188[a] 3,026	α1A-178,[b] β5-188[a] 3,100
Water molecules	9	114
Carbohydrates	1 (Asnβ19)	0
Refinement resolution	27.0 to 2.60 Å	24.0 to 2.40 Å
R_{free} for F≥ 0σ (F ≥ 2σ)	32.0% (31.1%)	30.8% (29.4%)
Last shell	45.6% (38.8%)	37.5% (33.3%)
R_{cryst} for F ≥ 0σ (F ≥ 2σ)	25.5% (24.6%)	25.3% (24.1%)
Last shell	41.2% (35.3%)	35.6% (31.0%)
<B>	51 Å^2	30 Å^2
rmsd bond length	0.012 Å	0.009 Å
rmsd bond angle	2.6°	1.8°
rmsd dihedral	29.2°	29.7°

[a] First two residues of an eight-residue tail (SSADLVPR), which remained after removal of an engineered leucine zipper by thrombin digestion (Scott et al., 1996), are also modeled.
[b] All eight residues of the thrombin-digested leucine zipper tail are also modeled.

further modified to encode either the OVA or HA peptide sequence attached by a six-residue linker (GSGSGS) to the first codon of the mature β chain. Both inserts were cloned into an expression vector with a metallothionein-driven promoter (Scott et al., 1998).

The I-A^d α chain and I-A^d β chain constructs and a neomycin-resistance gene construct were transfected into *Drosophila melanogaster* S2 cells. Soluble I-A^d was isolated from the growth media using Ni-NTA technology (Qiagen, Santa Clara, California). The protocols for protein expression, isolation, and purification have been described previously (Scott et al., 1998). Crystals were grown in sitting drops by the vapor diffusion method (Stura and Wilson, 1992) at a fixed temperature of 22°C using protein concentrations ranging from 5 to 9 mg/ml. For low-temperature data collection, crystals were transferred into the same mother liquor, with 30% glycerol added as cryoprotectant prior to cryocooling.

Data Collection and Space Group Determination

As previously reported, a molecular replacement solution was found for the I-A^d–OVA complex using data collected from one crystal at room temperature (Scott et al., 1998) and HLA-DR1 (Stern et al., 1994; Protein Data Bank, Brookhaven National Laboratory [PDB] accession code 1DLH) as a molecular probe. Higher resolution oscillation data for both complexes were collected at the Stanford Synchrotron Radiation Laboratories using the in-house open-flow low-temperature cryostat to flash-cool the crystal to approximately 95°K. Data were collected on a MAR area detector and were indexed and scaled using DENZO (Otwinowski, 1993). Consistent with the space group determination for the room temperature data, the highest symmetry space group found with DENZO for the I-A^d–OVA data was primitive tetragonal. Using AMoRe (Navaza, 1994), the partially refined I-A^d–OVA model was used as a search model for a molecular replacement solution with the cryocooled data set indexed in $P4_12_12$. The best rotation translation solution had a correlation coefficient of 66.7% and an R_{cryst} of 0.37 ($R_{cryst} = \Sigma_{hkl}|Fo-Fc|/\Sigma_{hkl}Fo$, where F_o and F_c are observed and calculated structure factors, respectively) compared to the next-best solution, which had a correlation coefficient of 22.1% and an R_{cryst} of 0.56. DENZO was also used to determine that the space group of I-A^d–HA was C2 and was verified by pseudoprecession analysis using XPREP (SHELXTL 5.03, Siemens Industrial Automation, Madison, WI, 1990–1995).

A molecular replacement solution was found for the I-A^d–HA complex using AMoRe and the partially refined I-A^d–OVA complex as a molecular probe.

Each complex was built independently. In the last round of building, the I-A^d–OVA and I-A^d–HA structures were superimposed and compared. Model building was done in O (Jones et al., 1991) using a combination of shake-omit $2F_o-F_c$ and F_o-F_c density maps. Refinement was carried out with XPLOR version 3.8 (Brünger, 1992). Before model building was begun, both complexes were first refined using whole-molecule and then domain rigid body refinement. For the I-A^d–OVA complex, five rounds of model building were carried out in conjunction with the slow-cool refinement protocol of XPLOR using all reflections between 8 and 2.6 Å. All reflections to 2.6 Å were used to calculate electron density maps. Electron density was seen for a single N-acetylglucosamine moiety at one of the three putative N-linked carbohydrate sites, and one sugar was built into this density. Subsequently, bulk solvent correction was applied to all reflections using XPLOR. Five rounds of model building combined with positional and B-value refinement were carried out. Water molecules were then identified from residual density greater than 2.2 σ in $2F_o-F_c$ maps using XPLOR. Each water molecule was checked for valid geometry, environment, and correct shape of density before proceeding to more rounds of model building, positional, and B-value refinement (Table 3).

Three rounds of model building and slow-cool refinement were done for the I-A^d–HA complex using all reflections between 8.0 and 3.0 Å, followed by four rounds of model building and slow-cool refinement with data between 8.0 and 2.4 Å. No convincing density was visible for any of the putative N-linked sugar sites. Bulk solvent correction was applied to all reflections, and several rounds of model

building and positional and B-factor refinement were done before water molecules were selected for inclusion in the model (Table 3).

Analysis and Visualization

The quality of the final structure was assessed with the program PROCHECK (Laskowski et al., 1993). The final I-A^d–OVA and I-A^d–HA models exhibit good stereochemistry, with 87.5% and 90.3% of the residues, respectively, in the most favored areas of the Ramachandran plot. The one outlier in both structures, β33Asn, corresponds to a type II′ β turn, as seen in other class II MHC structures. The likelihood of correct I-A^d–peptide conformation was also checked using ERRAT (Colovos and Yeates, 1993), which determines the probability of pairwise interactions using a nine-residue sliding window. Atomic coordinates of class II molecules for structural comparisons were obtained from the PDB, from Daved Fremont (Columbia University, New York, NY) (I-E^k) or Don Wiley (Harvard University, Cambridge, MA) (DR3-CLIP). Structural superposition was performed using the program MIDAS (Ferrin, 1988) and OVRLAP (Rossmann and Argos, 1975). Superposition of the MHC class II structures was done using residues in the β-sheet floor of the peptide-binding groove. The specific residues were α18–26, α29–34, β24–32, and β37–42, corresponding to the β strands that are conserved in all class II MHC structures. Cavities formed between MHC and peptide were identified using MSMS (Sanner et al., 1996) with a probe radius of 1.4 Å. For cavity analysis, the peptide in each MHC class II–peptide complex was changed to a polyglycine chain, and the probe was used to identify all cavities between MHC and polyglycine peptide that could be used as pockets for peptide side chains. The location of the pockets with respect to the peptide was visualized using AVS (Advanced Visual Systems, Wiltham, MA). GRASP (Nichols et al., 1991) was used to analyze buried surfaces and to view surface electrostatics. All images were produced using AVS. Coordinates have been deposited in the PDB with accession codes 1IAD (I-A^d–OVA) and 2IAD (I-A^d–HA) and will be available until their release by the PDB from wilson@scripps.edu.

Acknowledgments

We thank Michael Pique, Brent Segelke, and Michel Sanner for assistance in graphics and protein analysis; Jeff Speir, Massimo Degano, Robyn Stanfield, Samantha Greasley, and Andreas Heine for valuable advice and assistance in computational analysis; Daved Fremont for the I-E^k coordinates and helpful discussions; and Don Wiley and Partho Ghosh for the DR3-CLIP coordinates. This work was supported by National Institutes of Health grant CA-58896 (I. A. W.) and R. W. Johnson Pharmaceutical Research Institute (L. T.). This is publication 11302-MB from The Scripps Research Institute.

Received December 2, 1997; revised January 9, 1998.

References

Bjorkman, P.J., Saper, M.A., Samraoui, B., Bennett, W.S., Strominger, J.L., and Wiley, D.C. (1987). Structure of the human class I histocompatibility antigen, HLA-A2. Nature *329*, 506–512.

Brown, J.H., Jardetzky, T., Saper, M.A., Samraoui, B., Bjorkman, P.J., and Wiley, D.C. (1988). A hypothetical model of the foreign antigen binding site of class II histocompatibility molecules. Nature *332*, 845–850.

Brown, J.H., Jardetzky, T.S., Gorga, J.C., Stern, L.J., Urban, R. G., Strominger, J.L., and Wiley, D.C. (1993). Three-dimensional structure of the human class II histocompatibility antigen HLA-DR1. Nature *364*, 33–39.

Brünger, A.T. (1992). X-PLOR, Version 3.1: A System for X-Ray Crystallography and NMR (New Haven, CT: Yale University Press).

Buerstedde, J.M., Nilson, A.E., Chase, C.G., Bell, M.P., Beck, B. N., Pease, L.R., and McKean, D.J. (1989). A beta polymorphic residues responsible for class II molecule recognition by alloreactive T cells. J. Exp. Med. *169*, 1645–1654.

Burmeister, W.P., Gastinel, L.N., Simister, N.E., Blum, M.L., and Bjorkman, P.J. (1994). Crystal structure at 2.2 Å resolution of the MHC-related neonatal Fc receptor. Nature *372*, 336–343.

Campbell, R.D., and Milner, C.M. (1993). MHC genes in autoimmunity. Curr. Opin. Immunol. *5*, 887–893.

Colovos, C., and Yeates, T.O. (1993). Verification of protein structures: patterns of nonbonded atomic interactions. Protein Sci. *2*, 1511–1519.

Cresswell, P. (1994). Assembly, transport, and function of MHC class II molecules. Annu. Rev. Immunol. *12*, 259–293.

Dessen, A., Lawrence, C.M., Cupo, S., Zaller, D.M., and Wiley, D.C. (1997). X-ray crystal structure of HLA-DR4 (DRA*0101, DRB1*0401) complexes with a peptide from human collagen II. Immunity *7*, 473–481.

England, R.D., Kullberg, M.C., Cornette, J.L., and Berzofsky, J.A. (1995). Molecular analysis of a heteroclitic T cell response to the immunodominant epitope of sperm whale myoglobin: implications for peptide partial agonists. J. Immunol. *155*, 4295–4306.

Ferrin, T.E. (1988). The MIDAS display system. J. Mol. Graphics *6*, 13–27.

Fremont, D.H., Matsumura, M., Stura, E.A., Peterson, P.A., and Wilson, I.A. (1992). Crystal structures of two viral peptides in complex with murine MHC class I H-$2K^b$. Science *257*, 919–927.

Fremont, D.H., Hendrickson, W.A., Marrack, P., and Kappler, J. (1996). Structures of an MHC class II molecule with covalently bound single peptides. Science *272*, 1001–1004.

Fremont, D.H., Monnaie, D., Nelson, C.A., Hendrickson, W.A., and Unanue, E.R. (1998). Crystal structure of I-A^k in complex with a dominant epitope of lysozyme. Immunity *8*, this issue, 305–317.

Gautam, A.M., Pearson, C., Quinn, V., McDevitt, H.O., and Milburn, P.J. (1995). Binding of an invariant-chain peptide, CLIP, to I-A major histocompatibility complex class II molecules. Proc. Natl. Acad. Sci. USA 92, 335–339.

Gerhard, W., Haberman, A.M., Scherle, P.A., Taylor, A.H., Palladino, G., and Caton, A.J. (1991). Identification of eight determinants in the hemagglutinin molecule of influenza virus A/PR/8/34 (H1N1) which are recognized by class II-restricted T cells from BALB/c mice. J. Virol. *65*, 364–372.

Ghosh, P., Amaya, M., Mellins, E., and Wiley, D.C. (1995). The structure of an intermediate in class II MHC maturation: CLIP bound to HLA-DR3. Nature *378*, 457–462.

Hill, C.M., Liu, A., Marshall, K.W., Mayer, J., Jorgensen, B., Yuan, B., Cubbon, R.M., Nichols, E.A., Wicker, L.S., and Rothbard, J.B. (1994). Exploration of requirements for peptide binding to HLA DRB1*0101 and DRB1*0401. J. Immunol. *152*, 2890–2898.

Hunt, D.F., Michel, H., Dickinson, T.A., Shabanowitz, J., Cox, A.L., Sakaguchi, K., Appella, E., Grey, H.M., and Sette, A. (1992). Peptides presented to the immune system by the murine class II major histocompatibility complex molecule I-A^d. Science *256*, 1817–1820.

Jardetzky, T.S., Gorga, J.C., Busch, R., Rothbard, J., Strominger, J.L., and Wiley, D.C. (1990). Peptide binding to HLA-DR1: a peptide with most residues substituted to alanine retains MHC binding. EMBO J. *9*, 1797–1803.

Jardetzky, T.S., Brown, J.H., Gorga, J.C., Stern, L.J., Urban, R. G., Strominger, J.L., and Wiley, D.C. (1996). Crystallographic analysis of endogenous peptides associated with HLA-DR1 suggests a common, polyproline II-like conformation for bound peptides. Proc. Natl. Acad. Sci. USA *93*, 734–738.

Jones, T.A., Zou, J.Y., Cowan, S.W., and Kjeldgaard, M. (1991). Improved methods for building protein models in electron density maps and the location of errors in these models. Acta Cryst. *A47*, 110–119.

Klein, J. (1986). Natural History of the Major Histocompatibility Complex (New York, NY: John Wiley and Sons).

König, R., Huang, L.Y., and Germain, R.N. (1992). MHC class II interaction with CD4 mediated by a region analogous to the MHC class I binding site for CD8. Nature *356*, 796–798.

Kouskoff, V., Korganow, A.S., Duchatelle, V., Degott, C., Benoist, C., and Mathis, D. (1996). Organ-specific disease provoked by systemic autoimmunity. Cell *87*, 811–822.

Kozono, H., White, J., Clements, J., Marrack, P., and Kappler, J. (1994). Production of soluble MHC class II proteins with covalently bound single peptides. Nature *369*, 151–154.

Laskowski, R.J., Macarthur, W., Moss, D., and Thorton, J. (1993). Procheck: a program to check stereochemical quality of protein structures. J. Appl. Cryst. *26*, 283–290.

Lechler, R.I., Sant, A.J., Braunstein, N.S., Sekaly, R., Long, E., and Germain, R.N. (1990). Cell surface expression of hybrid murine/human MHC class II $\beta\alpha$ dimers: key influence of residues in the amino-terminal portion of the β 1 domain. J. Immunol. *144*, 329–333.

Lee, J.M., McKean, D.J., and Watts, T.H. (1991). Functional mapping of MHC class II polymorphic residues: the alpha-chain controls the specificity for binding an Ad-versus an Ak-restricted peptide and the β-chain region 65–67 controls T cell recognition but not peptide binding. J. Immunol. *146*, 2952–2959.

Matsumura, M., Fremont, D.H., Peterson, P.A., and Wilson, I.A. (1992). Emerging principles for the recognition of peptide antigens by MHC class I molecules. Science *257*, 927–934.

Murthy, V.L., and Stern, L.J. (1997). The class II MHC protein HLA-DR1 in complex with an endogenous peptide: implications for the structural basis of the specificity of peptide binding. Structure *5*, 1385–1396.

Nalefski, E.A., Shaw, K.T., and Rao, A. (1995). An ion pair in class II major histocompatibility complex heterodimers critical for surface expression and peptide presentation. J. Biol. Chem. *270*, 22351–22360.

Navaza, J. (1994). AMoRe: an automated package for molecular replacement. Acta. Cryst. *A50*, 157–163.

Nelson, C.A., Viner, N., Young, S., Petzold, S., Benoist, C., Mathis, D., and Unanue, E.R. (1996). Amino acid residues on the I-A^k α-chain required for the binding and stability of two antigenic peptides. J. Immunol. *156*, 176–182.

Nichols, A., Sharp, K.A., and Honig, B. (1991). Protein folding and association: insights from the interfacial and thermodynamic properties of hydrocarbons. Proteins *11*, 281–296.

Otwinowski, Z. (1993). Data collection and processing. In Proceedings of the CCP4 Study Weekend, L. Sawyer, P.R. Evans, and A.G.W. Leslie, eds. (Daresbury, UK: SERC Daresbury Laboratory), pp. 80–86.

Paliaksis, K., Routsias, J., Petratos, K., Ouzounis, C., Kokkinidis, M., and Papadopoulos, G.K. (1996). Novel structural features of the human histocompatibility molecules HLA-DQ as revealed by modeling based on the published structure of the related molecule HLA-DR. J. Struct. Biol. *117*, 145–163.

Rammensee, H.G., Friede, T., and Stevanoviic, S. (1995). MHC ligands and peptide motifs: first listing. Immunogenetics *41*, 178–228.

Rossmann, M.G., and Argos, P. (1975). A comparison of the heme binding pocket in globins and cytochrome b5. J. Biol. Chem. *250*, 7525–7532.

Runnels, H.A., Moore, J.C., and Jensen, P.E. (1996). A structural transition in class II major histocompatibility complex proteins at mildly acidic pH. J. Exp. Med. *183*, 127–136.

Sanner, M.F., Olson, A.J., and Spehner, J.-C. (1996). Reduced surface: an efficient way to compute molecular surfaces. Biopolymers *38*, 305–320.

Sant, A.J., Hendrix, L.R., Coligan, J.E., Maloy, W.L., and Germain, R.N. (1991). Defective intracellular transport as a common mechanism limiting expression of inappropriately paired class II major histocompatibility complex alpha/beta chains. J. Exp. Med. *174*, 799–808.

Saper, M.A., Bjorkman, P.J., and Wiley, D.C. (1991). Refined structure of the human histocompatibility antigen HLA-A2 at 2.6 Å resolution. J. Mol. Biol. *219*, 277–319.

Scott, B., Liblau, R., Degermann, S., Marconi, L.A., Ogata, L., Caton, A.J., McDevitt, H.O., and Lo, D. (1994). A role for non-MHC genetic polymorphism in susceptibility to spontaneous autoimmunity. Immunity *1*, 73–83.

Scott, C.A., Garcia, K.C., Carbone, F.R., Wilson, I.A., and Teyton, L. (1996). Role of chain pairing for the production of functional soluble IA major histocompatibility complex class II molecules. J. Exp. Med. *183*, 2087–2095.

Scott, C.A., Garcia, K.C., Peterson, P.A., Wilson, I.A., and Teyton, L. (1998). Engineering protein for x-ray crystallography: the murine major histocompatiblity complex class II molecule I-A^d. Protein Sci. *7*, 413–418.

Sette, A., Buus, S., Colon, S., Smith, J.A., Miles, C., and Grey, H.M. (1987). Structural characteristics of an antigen required for its interaction with Ia and recognition by T cells. Nature *328*, 395–399.

Sette, A., Buus, S., Colon, S., Miles, C., and Grey, H.M. (1988). I-A^d-binding peptides derived from unrelated protein antigens share a common structural motif. J. Immunol. *141*, 45–48.

Sette, A., Buus, S., Appella, E., Smith, J.A., Chesnut, R., Miles, C., Colon, S.M., and Grey, H.M. (1989a). Prediction of major histocompatibility complex binding regions of protein antigens by sequence pattern analysis. Proc. Natl. Acad. Sci. USA *86*, 3296–3300.

Sette, A., Buus, S., Colon, S., Miles, C., and Grey, H.M. (1989b). Structural analysis of peptides capable of binding to more than one Ia antigen. J. Immunol. *142*, 35–40.

Sette, A., Lamont, A., Buus, S., Colon, S.M., Miles, C., and Grey, H. M. (1989c). Effect of conformational propensity of peptide antigens in their interaction with MHC class II molecules: failure to document the importance of regular secondary structures. J. Immunol. *143*, 1268–1273.

Sette, A., Sidney, J., Albertson, M., Miles, C., Colon, S.M., Pedrazzini, T., Lamont, A.G., and Grey, H.M. (1990). A novel approach to the generation of high affinity class II-binding peptides. J. Immunol. *145*, 1809–1813.

Sette, A., Southwood, S., Miller, J., and Appella, E. (1995). Binding of major histocompatibility complex class II to the invariant chain-derived peptide, CLIP, is regulated by allelic polymorphism in class II. J. Exp. Med. *181*, 677–683.

Shimonkevitz, R., Colon, S., Kappler, J.W., Marrack, P., and Grey, H.M. (1984). Antigen recognition by H-2-restricted T cells. II. A tryptic ovalbumin peptide that substitutes for processed antigen. J. Immunol. *133*, 2067–2074.

Stern, L.J., Brown, J.H., Jardetzky, T.S., Gorga, J.C., Urban, R.G., Strominger, J.L., and Wiley, D.C. (1994). Crystal structure of the human class II MHC protein HLA-DR1 complexed with an influenza virus peptide. Nature *368*, 215–221.

Stern, L.J., and Wiley, D.C. (1994). Antigenic peptide binding by class I and class II histocompatibility proteins. Structure *2*, 245–251.

Stura, E.A., and Wilson, I.A. (1992). Seeding techniques. In Crystallization of Nucleic Acids and Proteins, A. Ducruix and A.D. Giege, eds. (Oxford, UK: Oxford University Press), pp. 99–126.

Tisch, R., and McDevitt, H. (1996). Insulin-dependent diabetes mellitus. Cell *85*, 291–297.

Wilson, I.A. (1994). Covalently-linked ligand stabilizes expression of heterodimeric receptor. Structure *2*, 561–562.

Wilson, I.A. (1996). Another twist to MHC-peptide recognition. Science *272*, 973–974.

Witt, S.N., and McConnell, H.M. (1994). Formation and dissociation of short-lived class II MHC-peptide complexes. Biochemistry *33*, 1861–1868.

Zeng, Z., Castaño, A.R., Segelke, B.W., Stura, E.A., Peterson, P.A., and Wilson, I.A. (1997). Crystal structure of mouse CD1: an MHC-like fold with a large hydrophobic binding groove. Science *277*, 339–345.